water

Article

Meteorological Effects of a Lake in A Permafrost Basin: Difference of Seasonal Freeze–Thaw Cycles in Hovsgol Lake and Darhad Basin, Northern Mongolia

Kazuo Takeda [1,*], Akifumi Sugita [2], Masato Kimura [1] and Maximo Larry Lopez Caceres [3]

[1] Department of Agro-environmental Science, Obihiro University of Agriculture and Veterinary Medicine, Obihiro 080-8555, Japan
[2] Kanki Co. Ltd., Sapporo 060-0004, Japan
[3] Faculty of Agriculture, Yamagata University, Tsuruoka 997-8555, Japan
* Correspondence: kazuotakeda9@gmail.com; Tel.: +81-79-562-8701

Abstract: The effects of the present global climate change appear more pronounced in high latitudes and alpine regions. Transitions zones, such as the southern fringe of the boreal region in northern Mongolia, are expected to experience drastic changes as a result. This area is dry and cold with forests forming only on the north-facing slopes of hills and grasslands distributing on the south-facing slopes, making it difficult for continuous forests to exist. However, in the Hovsgol Lake Basin, there is a vast continuous pure forest of Siberian larch (*Larix sibirica*). In other words, the lake water thawing/freezing process may have created a unique climatic environment that differs with the climate of the adjacent Darhad Basin, where no lake exists. Thus, in order to compare the effect of the thawing/freezing dynamics of lake water and the active layer on the thermal regime at each basin, respectively, temperatures were simultaneously measured. The Darhad Basin has similar latitude, topography, area, and elevation conditions. As expected, the presence of the lake affected the annual temperature amplitude, as it was 60% of that in the Darhad Basin. The difference in the seasonal freeze–thaw cycles of the lake and the active layer caused a significant difference in the thermal regime, especially in winter.

Keywords: Mongolia; Hovsgol Lake; Darhad Basin; continuous permafrost; freeze–thaw cycles; meteorological effects; lake water; active layer

check for updates

Citation: Takeda, K.; Sugita, A.; Kimura, M.; Caceres, M.L.L. Meteorological Effects of a Lake in A Permafrost Basin: Difference of Seasonal Freeze–Thaw Cycles in Hovsgol Lake and Darhad Basin, Northern Mongolia. *Water* **2022**, *14*, 2785. https://doi.org/10.3390/w14182785

Academic Editors: Wojciech Dobinski and Aizhong Ye

Received: 21 July 2022
Accepted: 2 September 2022
Published: 7 September 2022

1. Introduction

The effects of the present global climate change appear to be more pronounced in high latitudes and alpine regions [1–7]. The effects are manifested in different processes of freezing and thawing of lakes and rivers with more variability in ice thickness and freezing periods [8,9]. Because the amount of latent heat from freezing and thawing is much greater in lakes than in warmer regions, such as mid-latitudes and low-latitudes, the effects of lakes on the surrounding environment, including their climatic, ecological, and hydrological characteristics, are also significant [9–15]. However, studies evaluating the impact of lakes on the environment based on field observations are limited. In particular, there are hardly any studies that have evaluated the impact of lakes on the environment compared to areas without lakes that are exposed to the same geographic conditions and can control the freezing and thawing processes of the active layer.

The Hovsgol Lake Basin is home to a vast pure forest of Siberian larch (*Larix sibirica*), which is rare in the Boreal region [16]. The Hovsgol area in the northernmost part of Mongolia, where the basin is located, is at the southern end of continuous permafrost and taiga zone extending from Eastern Siberia, where a pristine natural environment remains. According to the local Hatgal weather station, the average annual temperature over the period 1973–2020 has been –4.0 °C, with an average annual precipitation of

294 mm, and snowfall during the winter months is low, with an average precipitation of 28 mm from October to March [17]. Due to the cold and dry climate, forests form on the north-facing slopes of mountains in the region, while grasslands spread on the south-facing slopes [18], preventing the formation of continuous forests. Forests outside the basin are mixed coniferous and broadleaf forests [19]. In the adjacent Darhad Basin, where no lake exists, the vegetation is a mixture of conifers such as larch (*Larix sibirica*), spruce (*Picea obovata*), and red pine (*Pinus sylvestris*) and broadleaf trees such as birch (*Betula pendula*) and poplar (*Populus tremula*) [20,21], while in the Hovsgol Lake Basin, vast pure larch forests are widespread. In other words, the differences in the biodiversity of vegetation between these two basins is likely driven by the presence of the lake in the Hovsgol Lake Basin, as well as its sensitivity to climate change.

In recent years, air temperatures in northern Mongolia have been on the rise. This has been particularly significant in the Hovsgol Lake Basin and Darhad Basin, as reported by the few long-term meteorological stations located in each site [1,17,22]. The impact on the sustainability of pure forests in this transition zone can be significant, since forests can be sensitive to permafrost thawing caused by enhanced drought or forest fires. Lake water has different freeze–thaw characteristics in comparison to soil active layers. These differences can also lead to an assessment of the lake water annual thermal variability on the surrounding environment. We conducted simultaneous observations of air temperature in the Hovsgol Lake Basin and the Darhad Basin, which are similar in terms of latitude, topography, basin bottom area, and elevation. In this study, we aimed at quantifying the differences in the air thermal regime caused by the lake water freezing and thawing in comparison to the freezing and thawing of soil active layers in the Darhad Basin. The results of this study are a rare case that highlights the importance of this area as an indicator of climate change, a source for improving the accuracy of lake environmental forecasts, and for assessing the resilience and vulnerability of lake environments in the short- and long-term future.

2. Methodology

2.1. Study Area

The Hovsgol region in northern Mongolia consists of a lake basin with the country's largest freshwater lake, Hovsgol Lake, and the Darhad Basin to the west is covered by steppe-forest vegetation. The two basins are both aligned at the same latitude, orthogonally to the 51st of north–south latitude (Figure 1). The elevation (MSL) of the lake is slightly higher at 1654 m than the latter basin bottom of 1540 m to 1600 m, and the areas of the lake and basin bottom are almost equal at 2750 km^2 and 2780 km^2, respectively, with much in common (Table 1) [23–26]. Hovsgol Lake, a fault lake, has a basin area of 1.8 times the area occupied by the lake, which is small compared to other lake basins (e.g., Lake Baikal, 18.1 times [27]). The average depth is 138 m, the maximum depth is 267 m, the freezing period is approximately six months from November/December to May/June, and the maximum ice thickness exceeds 1 m [28,29]. Water transparency is not known from measurements but is thought to be comparatively high due to the lack of human activity and the fact that water from the Egin River at the southern end flows into Lake Baikal (elevation 456 m), which has high transparency downstream. To the west, the Hovsgol Lake Basin is bordered by a 3000 m high mountain range separating it from the Darhad Basin to the north by a 3000 m high mountain range on the Russian border and to the east by 2000 m high mountains. In contrast, the Darhad Basin is surrounded by mountains at elevations from 2500 m to over 3000 m. At the bottom of the basin, vast, flat grasslands spread over 100 m thick permafrost [30], and in the northern part, small lakes and marshes are scattered, showing traces of former glacial dammed lakes [24,26]. Again, the forest limit is around 2300 m.

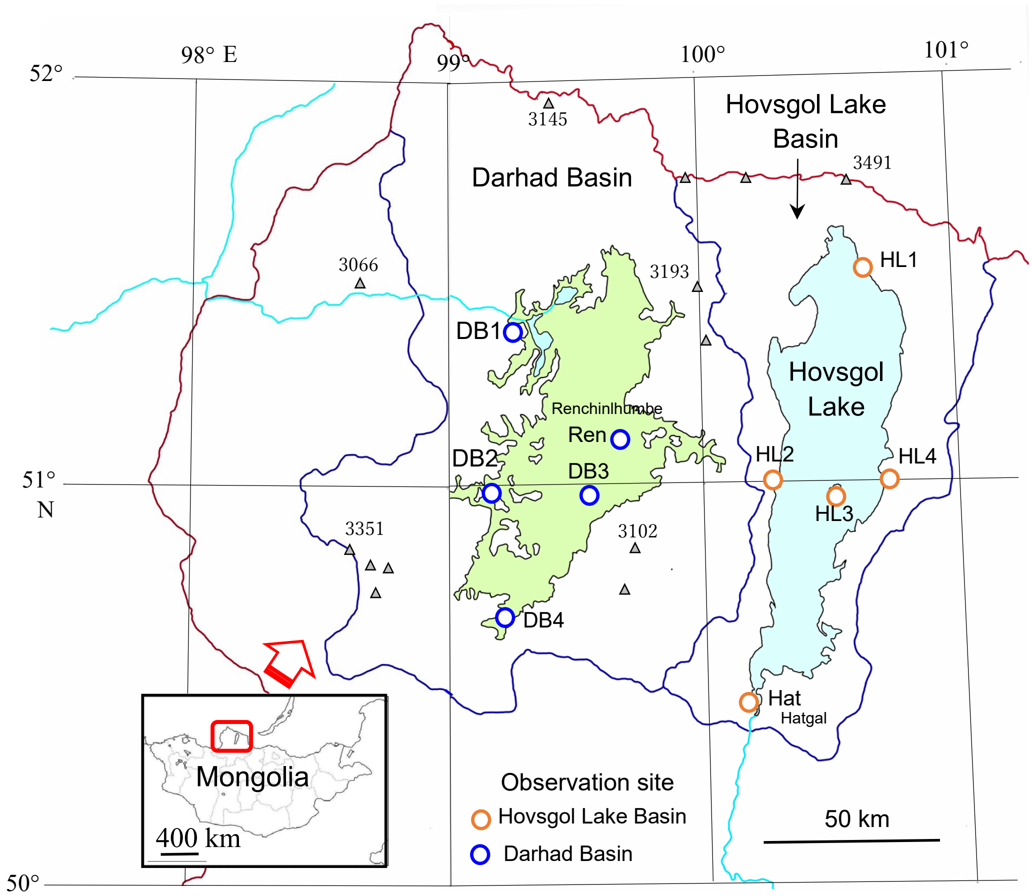

Figure 1. Location of observation sites in Hovsgol Lake Basin and Darhad Basin, northernmost Mongolia. The light blue area shows Hovsgol Lake, and the light blue lines represent the outflow river. The green area shows Darhad Basin drawn by the 1600 m height contour. The dark red line marks the border with Russia. The area bounded by dark blue lines and the border indicates the catchment area of each basin. The Δ symbols are some of mountains above 3000 m in height with number of the height.

Table 1. Characteristic features of the study area.

Parameter	Hovsgol Lake	Darhad Basin
Latitude	50°30′ N–51°35′ N * (1)	50°37′ N–51°32′ N
Area, km^2	2750 * (2)	2780 * (2)
Dimensions		
N–S, km	136 * (3)	100 * (4)
E–W, km	36.5 * (3)	40 * (4)
Altitude, m a.s.l.	1645 * (2)	1540–1600 * (2)
Status	Lake * (2)	Dry Basin * (2)

* (1) [23], * (2) [24] the area refers to the bottom of the basin, * (3) [25], * (4) [26].

2.2. Survey and Analysis

We compared the differences in thermal regimes by a series of measurements of air, ground, and water temperature. The set of available data included air temperature data from Renchinlhumbe weather station and from Hatgal weather station, including the start date of lake freezing, date and amount of maximum ice thickness, and date of completion of lake ice thawing, water temperature etc., that were collected [17,28]. The additional information, except air temperature, was obtained from a water level station on the lake shore near the southern end of Hovsgol Lake, 4 km north of the weather station. The ice thickness was measured by station personnel at a fixed point approximately 1 km offshore. The air temperature T_a (°C) were observed hourly at each of the five locations in the Hovsgol Lake Basin (HL) and Darhad Basin (DB) (Figure 1, HL: HL1–HL4 and Hatgal (Hat) and DB: DB1–DB4 and Renchinlhumbe (Ren), respectively) from August 2000 to October 2015, using sensors (TR-51, T&D) with built-in data loggers. The sensors were placed facing north in the trees generally 2 m–3 m above the ground to prevent loss. Ground temperature was measured at DB3 at D_{30} (0.3 m depth: August 2004 to August 2008), and a field survey (thickness of active layer and soil survey) was conducted in August 2003. The daily mean temperature T_m (°C), calculated from T_a, represents the absolute accumulated value TT (°C-days) and was calculated as a 5-day moving averages. The daily ice thickness or the freezing depth D (m) of the active layer was calculated using the integrated value of air temperature, an empirical equation based on the Stefan's solution [31] derived from the unsteady heat conduction equation with a phase change for freezing,

$$D = \alpha \sqrt{TT}, \tag{1}$$

where α: constant.

$$TT = | \Sigma T_m |, \tag{2}$$

For the calculation of the freezing process, lake ice thickness $D = D_i$ (m), the freezing depth of the active layer $D = D_F$ (m), and the constant for freezing $\alpha = \alpha_F$ were used. Daily lake ice thawing thickness and active layer thickness were also calculated by applying Equation (1) [32,33]. For the calculation of the thawing process, lake ice, or frozen layer thawing thickness $D = D_T$ (m), freezing-related constant $\alpha = \alpha_T$ was used. The T_a data for each area were used to estimate the freezing index (FI (°C-days)) and the thawing index (TI (°C-days)) [30,32,33]. These indices were calculated using the following equation [34,35]:

$$FI = \left| \int_{d_{max}}^{d_{min}} T_m \, d \right|, \tag{3}$$

$$TI = \int_{d_{min}}^{d_{max}} T_m \, d, \tag{4}$$

where $T_m(d)$ is the daily average temperature on day d, and d_{max} and d_{min} represent the day when T_m shows the annual minimum and maximum, respectively, during the targeted period.

The latent heat E (MJ m^{-2}) associated with freezing or thawing of lake water, active layer, lake ice, or frozen soil is,

$$E = \mathrm{L} \cdot \beta \cdot D, \tag{5}$$

where L is latent heat of freezing (333.6 MJ-t^{-1}), β is a constant that varies with the object, and D is thickness of freezing or thawing (m).

(i) Latent heat of freezing of lake water or thawing of lake ice E_i (MJ-m^{-2}); (Equation (5), where β (= ρ_i: density of ice 0.917 t-m^{-3}) [36].
(ii) Latent heat quantity E_s (MJ-m^{-2}) associated with freezing of active layer; (Equation (5), where β (= $\theta \times \rho_w$, θ: volumetric water content 0.30 (m^3-m^{-3}), ρ_w: density of water 0.9998 t-m^{-3}) [36].
(iii) Latent heat of melting of frozen soil E_s (MJ-m^{-2}); (Equation (5), β (= $\theta \times \rho_i \times \Upsilon$, θ: volumetric water content 0.30 (m^3-m^{-3}), ρ_i: density of ice 0.917 t-m^{-3}, Υ: freezing (volumetric expansion rate of water at time of freezing = 1.09).

Positive values of E indicate heat generation due to freezing, and negative values indicate heat absorption due to thawing. The volumetric water content is based on field surveys.

3. Results and Discussions

3.1. Temperature Difference between Hovsgol Lake Basin and Darhad Basin

The basic temperature differences between the Hovsgol Lake Basin and Darhad Basin are shown in terms of integrated temperatures. To compare the degree of coldness and warmth from the temperature results observed from October 2006 to October 2007 at the five locations in each basin, the freezing index (*FI*) (Figure 2a) and thawing index (*TI*) (Figure 2b) were calculated from Equations (3) and (4), respectively [37]. The maximum *FI* for HL was 2106 °C·days for Hat (Hatgal), and the minimum was 1581 °C·days for HL3, while for DB the maximum was 3299 °C·days for Ren (Renchinlhumbe), and the minimum was 2891 °C·days for DB4. The mean value in HL was 59% of that in DB. The lowest HL, HL3, which is considered to be greatly influenced by lake water, was 50% of that in DB3. On the other hand, the maximum *TI* for HL was 1632 °C·days for HL1 and the minimum 1341 °C·days for HL4, while the maximum *TI* for DB was 1896 °C·days for DB4, and the minimum *TI* was 1683 °C·days for Ren. The average value of HL was 86% of that in DB, and in HL3 it was 84% of that in DB3. The result indicates that the presence of the lake water moderated winter temperatures in HL by approximately half compared to DB and made it cooler with less warmth in summer.

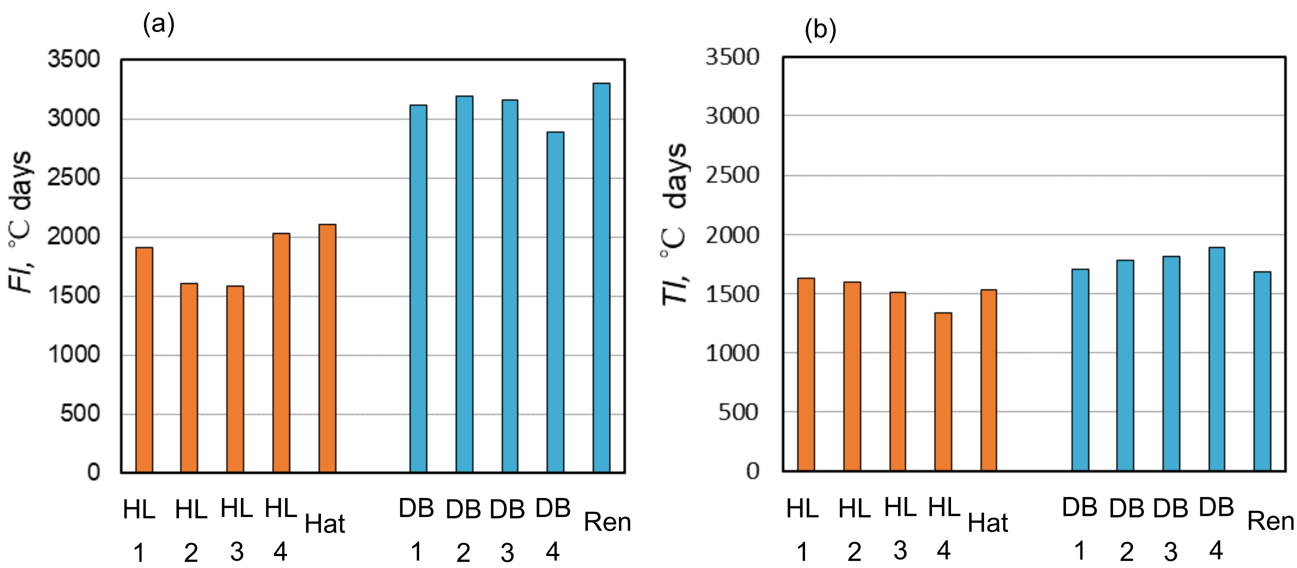

Figure 2. (**a**) Freezing (*FI*) and (**b**) thawing indices (*TI*) in Hovsgol Lake Basin and in Darhad Basin.

HL3 and DB3, located in the center of HL and DB, were representative of each basin. Long-term temperatures in the two basins are shown in Figure 3. Observations were made from 12 August 2000 to 28 November 2009 in HL3 and from 3 March 2004 to 7 October 2015 in DB3 and over a period of 5 years and 9 months from 3 March 2004 to 28 November 2009 in both basins. The measurements were conducted simultaneously. The annual maximum temperature during the observation period were 28.7 °C at 13:00 on 20 July 2001 in HL3 and 37.1 °C at 17:00 on 11 August 2007 in DB3. On the other hand, the annual minimum temperature was –36.6 °C at 10:00 on 26 January 2005 in HL3 and –52.4 °C at the same time in DB3, with DB3 being 15.8 °C lower than HL3. Overall, temperatures were lower in HL than in DB during summer and significantly higher in HL than in DB during winter. The correlation between temperatures between HL3 (island) and Hatgal (water level station) over a four-year period (30 August 2005–28 November 2009) was calculated.

$$y = 0.77x + 0.97\ (R^2 = 0.92,\ p < 0.01,\ N = 36{,}195) \tag{6}$$

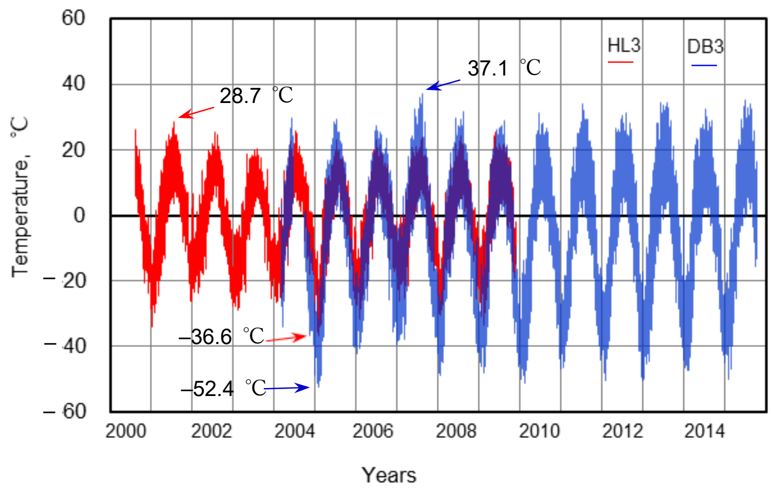

Figure 3. Air temperature changes at sites HL3 and DB3.

Here, y is T_a in HL3, and x is T_a at Hatgal. Island temperatures were approximately 80% of that in Hatgal. Similarly, the correlation of temperatures from hourly simultaneous observations at Darhad Basin Central, DB3, and Renchinlhumbe weather station yard (observed by loggers in the yard) over a period of 8 years (15 September 2007–5 October 2015) yielded

$$y = 1.05\ x + 0.15\ (R^2 = 0.99, p < 0.01, N = 70{,}562), \tag{7}$$

Here, y is T_a in DB3, and x is T_a at Renchinlhumbe. The difference between the two was small. Furthermore, from the simultaneous observations of HL3 and DB3 from 3 March 2004 to 28 November 2009, the correlation of temperatures was examined and found to be

$$\mathrm{y} = 0.60\ \mathrm{x} + 2.28\ (\mathrm{R}^2 = 0.89, \mathrm{p} < 0.01, \mathrm{N} = 47{,}689), \tag{8}$$

Here, y is T_a of HL3, and x is T_a of DB3. In other words, the presence of the lake reduced the amplitude of temperature in DB3 by approximately 60% in comparison to HL3.

3.2. Freeze–Thaw Characteristics of Lake Water and Active Layer

In order to identify the freeze–thaw period for lake water and the active layer, we compared meteorological data for the two basins: temperature changes observed in Lake Hovsgol basin HL3 and Darhad basin DB3 from 2007 to 2008 (Figure 4a,b) with H1–H5 and D1–D4 (Table 2). These are based on temperature analyses and observations related to the Hatgal and Renchinlhumbe weather stations.

Specific freeze–thaw events were followed. As shown in Figure 4a, ice melting at HL3 began on 16 April 2007 (H1) and was completed on 25 May 2007 (H2). After that, the air temperature was generally higher than the water temperature until 14 August (H3), and the temperature became lower than the water temperature until 18 November (H4), when the lake water began to freeze; from H4 to 29 February (H5), when the maximum lake ice thickness was reached, the lake ice grew; from H5 to 11 April 2008, when the lake ice melt began (H1), the ice maintained its thickness with the temperature change, whereas, at DB3, the frozen ground began to thaw from the surface on 5 April 2007 (D1), and the thawing continued until the maximum active layer thickness of 1.02 m on 16 August 2007 (D2). Here, the 2007 maximum active layer thickness of DB3 was calculated based on the 26 August 2003 field survey; after D2, the active layer began to freeze from the bottom due to the cold heat of the permafrost [37,38], and as shown in Figure 5, after a while the air temperature dropped, and freezing also began from the top of the ground on October 4 (D3). The ratio of the final freezing thickness from the top to the bottom and that from the bottom to the top is 4:1 based on permafrost observations and simulations [33], which means that 0.82 m from the top began to freeze at D3. Finally, freezing of the active layer was completed on 9 December, D4. Thereafter, the frozen layer continued to retain itself through repeated cooling and temperature changes until 11 April 2008 (D1).

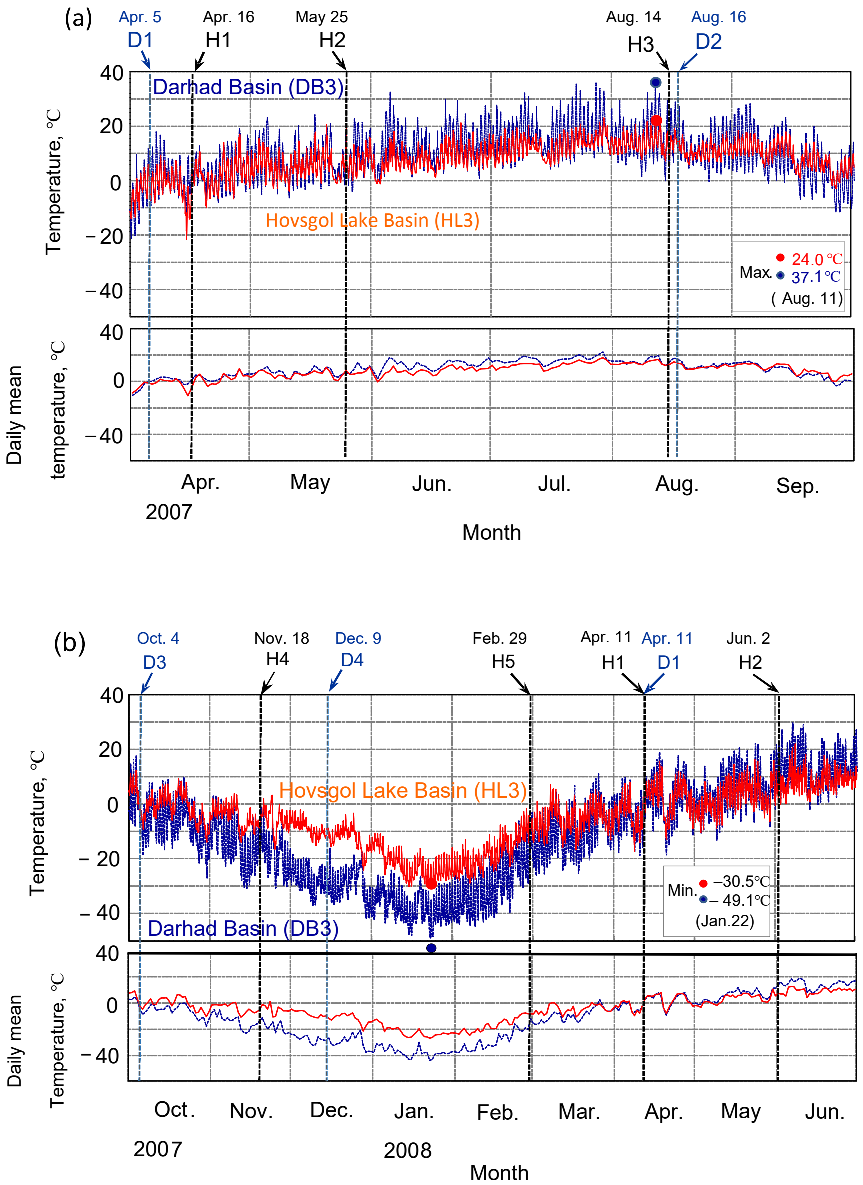

Figure 4. (**a**) Air temperature changes and meteorological events on thawing process of lake ice in Hovsgol Lake Basin (red line) or frozen ground in Darhad Basin (blue line). (**b**) Air temperature changes and meteorological events on freezing process of lake water in Hovsgol Lake Basin (red line) or active layer in Darhad Basin (blue line). See Table 2 for symbols.

The temperature difference due to the freeze–thaw event is noted. Comparing both HL3 and DB3 temperatures during the period from H1 to H2 with lake ice, it was found that there was no significant difference in the daily mean temperatures, although there were daily differences. However, during the period from H2 to H3 without lake ice, DB3′s mean temperature was higher than that at HL3, and the difference between the two mean temperatures became smaller from H3 to D3, but after D3, HL3 was higher than DB3 and the difference became larger, reaching a maximum around D4; from H5 to H1, the difference between the two almost disappeared.

Table 2. List of meteorological events on freeze–thaw cycles of lake water in Hovsgol Lake Basin or active layer in Darhad Basin. Symbols and dates correspond to Figure 4a,b; (date) is not shown.

Symbol	Meteorological Events	Date of Onset	
		2007	2008
Hovsgol Lake Basin (HL3)			
H1	Thaw start of lake ice	16 April	11 April
H2	Thaw end of lake ice	25 May	2 June
H3	Air temperature decreases below lake water temperature *	14 August	(14 August)
H4	Freeze start of lake water	18 November	(24 October)
H5	Maximum thickness of lake water	(10 February)	29 February
Darhad Basin (DB3)			
D1	Thaw start at the top of frozen ground	5 April	11 Aprilie
D2	Maximum thickness of active layer (freeze start at the bottom of active layer)	16 August	(14 August)
D3	Freeze start at the top of active layer	4 October	(30 September)
D4	Freeze end of active layer	9 December	(12 December)

*: The last day when 5-day moving average of daily temperature is above the lake water temperature of 13.6 °C (average of August monthly water temperature for 13 years).

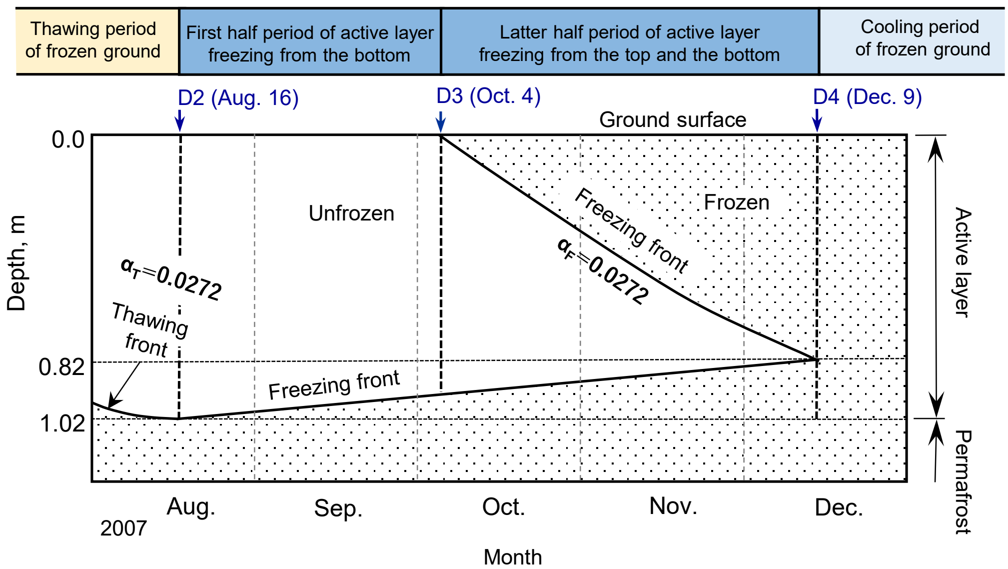

Figure 5. Schematic drawings of active layer on freeze–thaw processes and of seasonal division in Darhad Basin.

3.3. Timing of Freeze–Thaw Events

When analyzing local climate change, it is important to be able to represent freeze–thaw events in lake water and active layers using existing meteorological data from local weather stations, as these can be used to reproduce past freeze–thaw events.

H1, H2, and H4, which characterize the meteorological environment of Hovsgol Lake Basin, are uniquely determined from weather station data. In the graph of integrated temperature *TT* by daily mean temperature T_m, H1 and D1, which are the start of melting of lake ice and frozen soil, can be determined from the annual minima. Similarly, D3 can be obtained from the maximum value. H3 can be obtained from the average water temperature data for the highest monthly temperature of August from March to November observed by the Hatgal weather station from 2001 to 2013, which has a 13-year average monthly temperature of 13.6 °C [28], and this value was used as the threshold value of H3, in order to equalize the daily average temperatures, the five-day average temperature was set at 13.6 °C. In 2007, H3 was set to 14 August, the lowest day of the summer when the five-day mean temperature exceeded 13.6 °C.

D2, when the maximum active layer thickness occurs, is expected to be near the end of the summer temperature peak. Summer ground temperatures have a time lag with air temperatures, and periods of high ground temperatures usually occur later than air temperature peaks. To find this date in DB3 even during periods of high ground temperatures, we considered a ground temperature of D_{30} at 0.3 m depth of 6.5 °C or higher, which lasted from 24 July to 19 August, where the 5-day average was higher. The last summer peak in 5-day average air temperatures occurred from 9 August to 16 August, with an above-average air temperature of 13.2 °C in August at the Renchinlhumbe weather station. During this period, air temperatures were generally 2 °C above the monthly average. The last day of the peak was 16 August at 15.2 °C. Since air temperatures dropped rapidly after that, we expect the maximum active layer thickness to have occurred around this time, and we set this date as D2 in 2007. Here, the maximum active layer thickness at D2 can be obtained from *TT*, if α_T was originally obtained, using Equation (1). Therefore, to obtain α_T at DB3, we used the results of the field survey on 26 August 2003, estimated using Equation (7) from the meteorological data from the Renchinlhumbe weather station, since there were no temperature measurements at DB3 in 2003. DB3 is located in a former river wetland, with an active layer thickness of 1.02 m, fine sandy soil, high groundwater table, volumetric water content θ 0.30, porosity 0.55, and wet density 1.5 t-m^{-3}. The integrated temperature *TT* of D1–D2 spent thawing the frozen soil was calculated using Equation (1), α_T = 0.0272. Using this α_T, the maximum active layer thickness of 1.02 m at D2 was calculated using Equation (1) with the 2007 D1–D2-integrated temperature *TT* in DB3.

Finally, D4, the date of completion of freezing of the active layer, was determined as follows. The active layer freezes to a depth of 0.82 m from the top at D3, as described above, and considering that D1, D2, and D3 were determined separately and that the moisture state of the active layer does not change between the thawing and freezing processes (α_F and α_T in Equation (1) are equal), the latent heat of freezing of the active layer from D2 to D4 was calculated as described below in Section 3.4. The latent heat is equal to the latent heat of thawing expended in D1 to D2 (Table 3). Here, for convenience, we replace the latent heat with the integrated temperature. The integrated temperature *TT* from D1 to D2 spent thawing the frozen soil was 1419.2 °C-day, and the active layer thickness at D2 was 1.02 m. Equation (1) and α_T = 0.0272 indicate that the *TT* required to freeze the active layer thickness of 0.82 m is 908.3 °C-day. Using α_F = 0.0272 in Equation (1) to trace the date of occurrence of 908.3 °C-day after D3, D4, the date of completion of the freezing of the active layer, is 9 December.

3.4. Differences in Latent Heat during Freezing and Thawing

Differences between lake ice and frozen soil thawing were examined in terms of latent heat absorption. For each melting process, the daily melt thickness ΔD (m) of the lake ice was calculated by Equation (1) as α_T = 0.0778 using the integrated temperature *TT* in Equation (2). The latent heat was calculated using ΔD with Equation (5) and plotted in Figure 6a. In HL, melting began on 16 April 2007 (H1) and ended on 25 May 2007 (H2), for a period of about 1.3 months with a total latent heat of -305.9 MJ-m^{-2} (Table 3). On the other hand, in DB, the thawing of the frozen soil began from the surface layer on 5 April 2007 (D1) and continued for about 4.5 months until 16 August 2007 (D2), when the maximum active layer thickness of 1.02 m occurred, and the total latent heat was -102.4 MJ-m^{-2}. At this time, using Equation (1), α_T = 0.0272. During this period, the daily latent heat fluctuated sharply between heat generation due to freezing (positive value) and heat absorption due to thawing (negative value) at the beginning of the period, but the values settled down in May, and the daily average values from 1 May to 25 May were −6.81 MJ-m^{-2} for HL and −0.804 MJ-m^{-2} for DB. Heat absorption remained 8.5 times greater in HL than in DB. Lake ice thawing was more active, whereas frozen soil thawing was slower, resulting in a large difference in thawing times.

Table 3. Special dates or values in freeze–thaw cycles.

Date or Value	Hovsgol Lake Basin	Darhad Basin
Thawing process		
Thaw start date	16 April 2007	5 April 2007
Thaw end date	25 May 2007	16 August 2007
Adsorbed duration of thawing latent heat, months	1.3	4.5
Total latent heat amount, MJ m^{-2}	–305.9	–102.4
Freezing process		
Freeze start date	18 November 2007	16 August 2007
Freeze end date	29 February 2008	9 December 2007
Released duration of freezing latent heat, months	3.5	3.8
Total latent heat amount, Mj m^{-2}	361.0	102.4

Similarly, the difference in freezing between the lake water and the active layer is seen in terms of latent heat generation. For each freezing process, the daily freezing thickness was determined using Equations (1) and (2), and the latent heat was calculated using Equation (5) and shown in Figure 6b. Lake freezing began on 18 November 2007 (H4) and continued for about 3.5 months until the maximum lake ice thickness (H5) on 29 February 2008, when the total latent heat was 361.0 MJ-m^{-2}. The total latent heat was 361.0 MJ-m^{-2}. On the other hand, the freezing of the active layer of DB started from the bottom (D3) at the maximum active layer thickness on 16 August 2007 (D2), from the surface on 4 October 2007 (D4), and completed on 9 December 2007 (D4). During the intervening 3.8 months, the total latent heat reached 102.4 MJ-m^{-2}. In particular, during the winter period from December 23 to February, after the winter solstice, no latent heat was generated in the DB, and a large amount of latent heat was generated in the HL. As a result, the freezing process did not differ much for the period of 3.5 months for HL3 and 3.8 months for DB3, but the onset period shifted significantly from November of the previous year to February of the following year and from August of the previous year to December of the previous year, respectively.

3.5. Differential Freeze–Thaw Effects of Lake and Active Layer on the Meteorological Environment

The freeze–thaw characteristics of the lake water and the active layer can be patterned into H1–H5 and D1–D4, respectively (Figure 7). There is a difference in the freezing period, with the freezing period H4–H5 occurring mainly from November to February in HL and D2–D4 occurring from August to December in DB; the annual minimum temperature on 22 January 2008 was −30.5 °C in HL and −49.1 °C in DB, showing a large difference in the latent heat due to the freezing of lake water in HL. In HL, latent heat is generated by lake water freezing, but in DB, no latent heat is generated, indicating the influence of lake water. On the other hand, the thawing of lake ice and frozen ground begins at about the same time of the year, April to May in H1–H2 and April to August in D1–D2, but the latter is about three times longer than the former, and this difference is apparent. Since lake ice is always floating on the lake surface, the thawing of lake ice is considered to occur from the upper surface due to solar radiation, wind, and rain, and from the lower surface due to the convection of lake water, and to be completed in a short time. However, the thawing of frozen soil depends on heat from the ground in one direction, and since unfrozen soil has a lower thermal conductivity than frozen soil [39], thawing is suppressed and proceeds slowly over a long period of time.

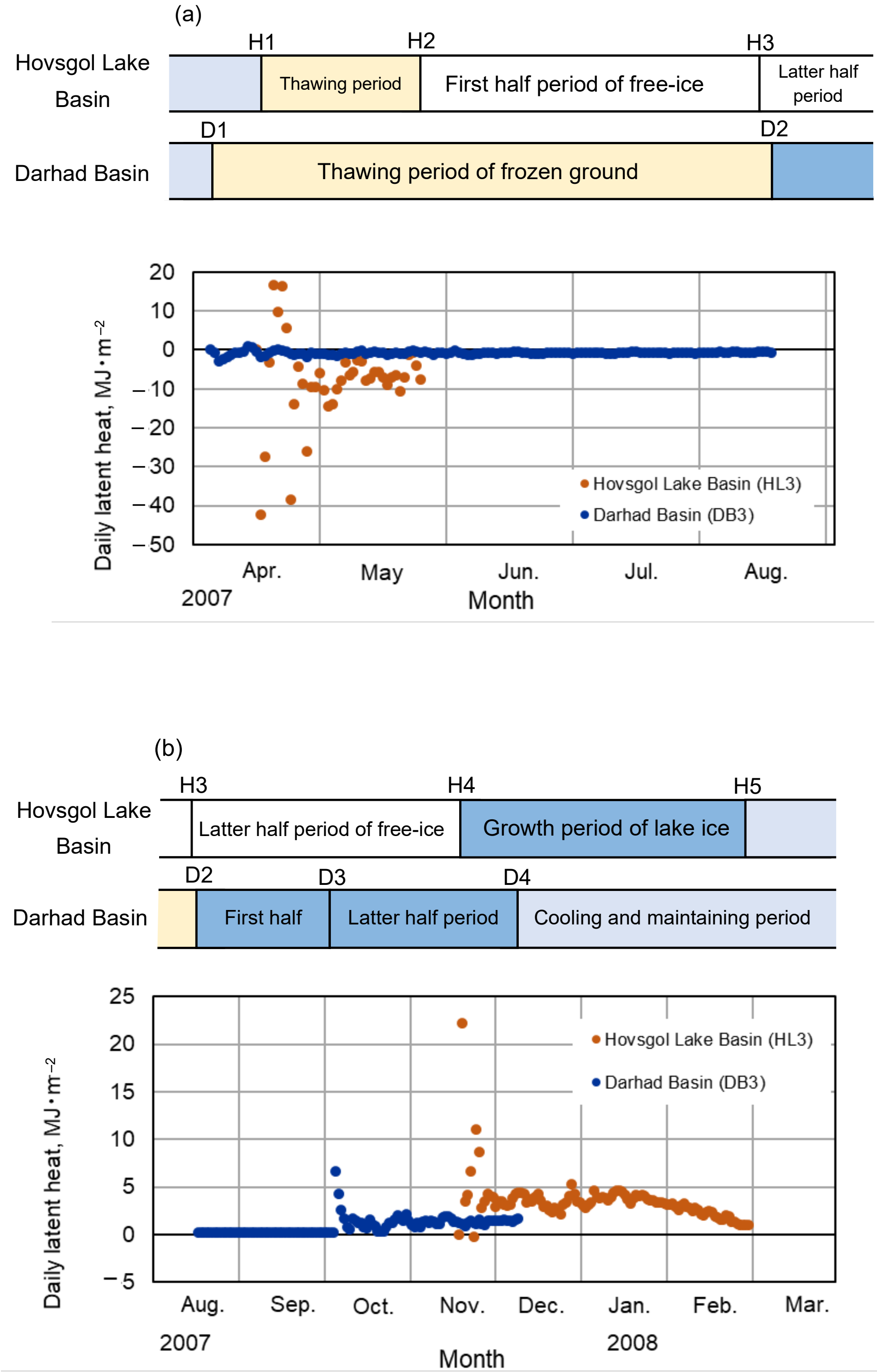

Figure 6. (**a**) Daily latent heat for lake ice or frozen ground in thawing process. Negative value is an adsorbed heat. (**b**) Daily latent heat for lake ice or active layer in freezing process. Positive value is a released heat.

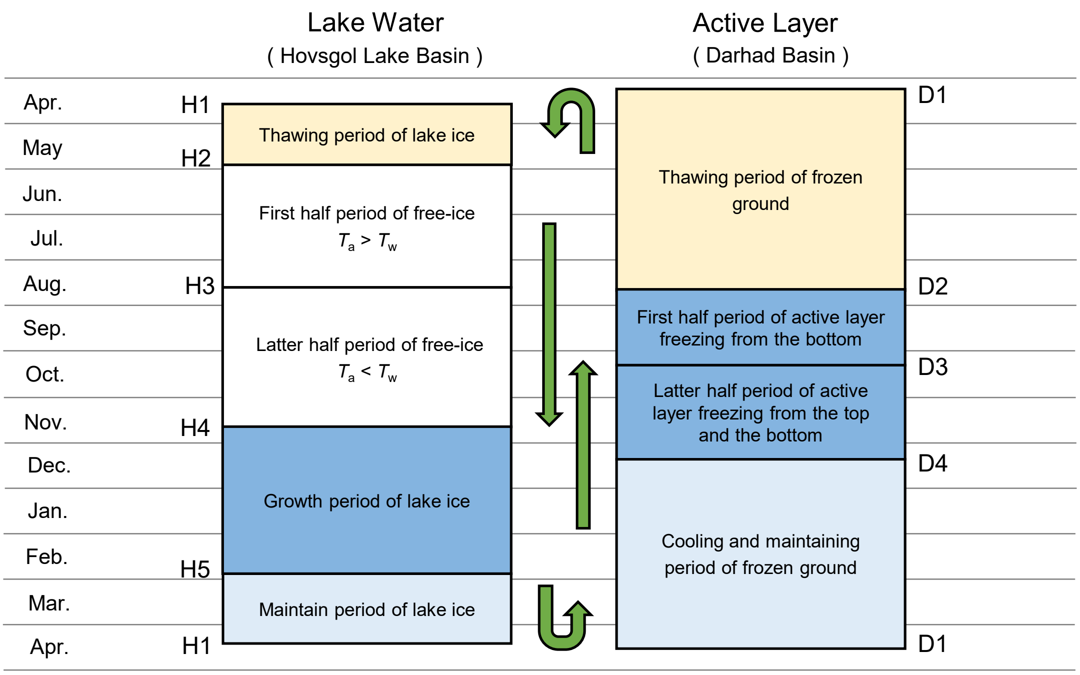

Figure 7. Seasonal pattern of freeze–thaw cycles for lake water and an active layer in a permafrost basin. T_a: air temperature; T_W: lake water temperature.

The freezing and thawing mechanisms of lake water are fundamentally different from those of the active layer. In lake freezing, winter cold determines the maximum thickness of lake ice, which is the dominant factor. Subsequent thawing is limited to the range of maximum lake ice thickness: the absolute value of the total latent heat associated with HL lake ice thawing in 2007 (-305.9 MJ-m^{-2}) is equal to the total latent heat that resulted in the maximum lake ice thickness in 2007, and the total latent heat associated with freezing in 2008, 361.0 MJ-m^{-2}, is equal to the absolute value of the total latent heat associated with thawing in that year. However, the thawing thickness of frozen soil depends on summer heat, and heat is dominant. Subsequent freezing is limited to the extent of the maximum active layer: the thawing of the frozen ground in 2007 was accompanied by a total latent heat of -102.4 MJ-m^{-2}, while the freezing of the active layer in that year generated the same amount of total latent heat of 102.4 MJ-m^{-2}, and the absolute values of both were the same. Therefore, the combination of lake water freezing and lake ice thawing and the combination of frozen soil thawing and the active layer freezing occur alternately, with the two occurring six months apart. Of the freezing and thawing, there is a time lag in the generation of latent heat, especially in freezing, which causes a large difference in winter temperatures, and the freeze–thaw action affects the climatic environment. If there were no lake water in the HL Basin, the freeze–thaw action would be very close to that observed in the DB active layer, and this difference could be one of the lake water effects on the climatic environment of the basin, which is located in the high-latitude permafrost zone.

One of the roles of inland lakes is to mitigate the effects of climate change. In this study, we quantitatively evaluated the lake's effects on the surrounding thermal regime and the difference of freeze–thaw mechanism, comparing the temperature difference between HL with lake water and DB without lake water. For example, in climate change prediction research, simulations that were previously conducted on a global scale have been replaced by regional-scale simulations that include lake water since around 2012, and the impact of lakes on the surrounding climate environment has also been studied at a higher resolution [40–43]. In such studies, the accuracy of simulation models is challenged when making climate change predictions, and observational data are used to validate lake water effects on the surrounding environment to enhance them. Therefore, the need for observational data on lake effects and long-term observations [e.g., 8] will increase in the future to predict the future of lake effects and to assess their resilience and vulnerability under climate change.

Finally, in addition to the freeze–thaw effect, another important factor affecting the climatic environment of the lake basin is the free-ice period from H2 to the first half of H3, which in 2007 was from 25 May to 14 August, and the mean temperature during the same period differed significantly from 10.7 °C in HL to 14.1 °C in DB. This period may have a significant impact on plant growth, especially because of the long hours of sunlight during this period, even during the year in high latitudes. As it was pointed out in the Introduction, the lake water forms a unique climatic environment and causes differences in vegetation, but this difference could be the subject for future study.

4. Conclusions

To evaluate the effect of lake water on the climatic environment in a high-latitude permafrost region, simultaneous temperature observations were conducted in two basins with similar latitude, elevation, area, and topography, which differ only in the presence or absence of lake water, in the Hovsgol Lake Basin and Darhad Basin, the latter not having a lake.

The results quantified the differences in the thermal regimes of the two basins as lake water effects on the surrounding climatic environment. The amplitude of temperature in the lake basin HL throughout the year was 60% of that in DB, indicating that the lake effect is responsible for the cool summer and mild winter climate. Comparison of the seasonal freeze–thaw cycle between the lake and the active layer showed a discrepancy in the timing of occurrence, even though the freezing period was almost equal in both. That is, the active layer took from August to December to freeze, while the lake water took from November to February. Lake water freezes mainly in midwinter and generates latent heat, while the active layer is already frozen at that time and does not generate latent heat. This difference was reflected in the annual minimum temperatures on 26 January 2005, which were −36.6 °C in HL and −52.4 °C in DB, a difference of 15.8 °C. The total latent heat generated by freezing was three times larger in the lake than in the active layer, whereas, although the onset time of thawing for the two was almost the same, the total latent heat absorbed by the lake ice was three times that of the frozen layer, but the duration of thawing was three times longer for DB than for HL due to the difference in thawing efficiency.

The Hovsgol Lake Basin, located in the northernmost part of Mongolia, has a cold arid climate, which prevents the formation of continuous forests. The vast Siberian larch forests exist in a highly fragile environment, which is created by precipitation accumulated during the summer under the cooler climate brought about by the lake effect. In the near future, global warming will alter the climatic environment by changing the heat and precipitation regimes, which will also affect vegetation. Therefore, continuous monitoring of the lake environment is necessary.

Author Contributions: K.T. participated in all the field surveys to set and manage field instruments; A.S. and M.L.L.C. participated in a field survey; K.T., A.S. and M.K. analyzed the data; K.T. and A.S. wrote the paper. All authors have read and agreed to the published version of the manuscript.

Funding: This study was financially supported by JSPS: KAKENHI (grant number 22405022) and the UGAS Dean Fund of Iwate University.

Institutional Review Board Statement: Not applicable.

Informed Consent Statement: Not applicable.

Data Availability Statement: Not applicable.

Acknowledgments: Special thanks to the late T. Kira, M. Nakagawa, and H. Fushimi (Biwa-Hovsgol Inter-lake Friendship Association) for providing the impetus for this research. I also thank J. Itoh, R. (Arima) Takagi, and M. (Imamura) Yamamoto, graduate students in Takeda laboratory of Obihiro University, and I would like to express my sincere gratitude to laboratory faculty members F. Tsuchiya, O. Tsuji, and T. Muneoka. I also thank the support of K.A. Chikita (Hokkaido University), Y. Nobori (Yamagata University), C. Mizota (Iwate University), S. Ishida (Hirosaki Univerasity), M. Byambasuren (PPRI, Mongloia), K. Saitoh (JAMSTEC), H. Yabuki (NIPR), and S. Miyazaki (Sonic Corporation).

Conflicts of Interest: The authors declare no conflict of interest.

References

1. Batima, P.; Natsagdorj, L.; Gombluudev, P.; Erdenetsetseg, B. Observed Climate Change in Mongolia. AIACC Work in Ulaanbaatar, Mongolia (published on-line by AIACC); 2005; Volume 25, p. 12.
2. Chapman, W.; Walsh, J. Recent variations of sea ice and air temperature in high latitudes. *Bull. Am. Meteorol. Soc.* **1993**, *74*, 33–47. [CrossRef]
3. Cohen, J.L.; Furtado, J.C.; Barlow, M.A.; Alexeev, V.A.; Cherry, J.E. Arctic warming, increasing snow cover and widespread boreal winter cooling. *Env. Res. Lett.* **2012**, *7*, 1–8. [CrossRef]
4. Cohen, J.L.; Furtado, J.C.; Barlow, M.; Alexeev, V.A.; Cherry, J.E. Asymmetric seasonal temperature trends. *Geophys. Res. Lett.* **2012**, *39*, 1–7. [CrossRef]
5. IPCC. *Climate Change 2013: The Physical Science Basis: Contribution of Working Group I to the Fifth Assessment Report of the Intergovernmental Panel on Climate Change*; Stocker, T.F., Qin, D., Plattner, G.K., Tignor, M., Allen, S.K., Boschung, J., Nauels, A., Xia, Y., Bex, V., Midgley, P.M., Eds.; Cambridge University Press: Cambridge, UK and New York, NY, USA, 2013; p. 1535.
6. IPCC. *Climate Change 2014: Synthesis Report: Contribution of Working Groups I, II and III to the Fifth Assessment Report of the Intergovernmental Panel on Climate Change*; Core Writing Team, Pachauri, R.K., Meyer, L.A., Eds.; IPCC: Geneva, Switzerland, 2014; p. 151.
7. IPCC. *Climate Change 2021: The Physical Science Basis, Contribution of Working Group 1 to the Sixth Assessment Report of Intergovernment Panel on Climate Change*; Cambridge University Press: Cambridge, UK and New York, NY, USA, 2021; pp. 3–32. [CrossRef]
8. Noori, R.; Bateni, S.M.; Saari, M.; Almazroui, M.; Haghighi, A.T. Strong warming rates in the surface and bottom layers of a boreal lake: Results from approximately six decades of measurements (1964–2020). *Earth Space Sci.* **2022**, *9*, 14. [CrossRef]
9. Noori, R.; Woolway, R.I.; Saari, M.; Merja, P.; Klove, B. *Six Decades of Thermal Change in A Pristine Lake Situated North of the Arctic Circle*; Earth and Space Science Open Archive: Published online, 2022; p. 21. [CrossRef]
10. Chikita, K.A.; Oyagi, H.; Aiyama, T.; Okada, M.; Sakamoto, H.; Itaya, T. Thermal Regime of a Deep Temperate Lake and Its Response to Climate Change: Lake Kuttara, Japan. *Hydrology* **2018**, *5*, 17. [CrossRef]
11. Elo, A.R.; Huttula, T.; Peltonen, A.; Virta, J. The effects of climate change on the temperature conditions of lakes. *Boreal Environ. Res.* **1998**, *3*, 137–150.
12. Schindler, D.W.; Bayley, S.E.; Parker, B.R.; Beaty, K.G.; Cruikshank, D.R.; Fee, E.J.; Schindler, E.U.; Stainton, M.P. The effects of climatic warming on the properties of boreal lakes and streams at the Experimental Lakes Area, northwestern Ontario. *Limnol. Oceanogr.* **1996**, *41*, 1004–1017. [CrossRef]
13. Sharkhuu, N. Recent Changes in the Permafrost of Mongolia. *Proc. Eighth Int. Conf. Permafr.* **2003**, *2*, 1029–1034.
14. Vavrus, S.J.; Wynne, R.H.; Foley, J.A. Measuring the sensitivity of southern Wisconsin lake ice to climate variations and lake depth using a numerical model. *Limnol. Oceanogr.* **1996**, *41*, 822–831. [CrossRef]
15. Yi, J.; Zhao, Y.; Shao, M.; Zhang, J.; Cui, L.; Si, B. Soil freezing and thawing processes affected by the different landscapes in the middle reaches of Heihe River Basin, Gansu, China. *J. Hydrol.* **2014**, *519*, 1328–1338. [CrossRef]
16. Kira, T.; Kusaka, S. Forests of the world today. *For. Environ.* **2006**, *6*, 170–179.
17. NOAA Satellite and Information Service. NCDC (National Climatic Data Center). Available online: https://www.ncdc.noaa.gov/cdo-web/ (accessed on 1 December 2021).
18. Ishikawa, M.; Sharkhuu, N.; Zhang, Y.; Kadota, T.; Ohta, T. Ground Thermal and Moisture Conditions at the Southern Boundary of Discontinuous Permafrost, Mongolia. Permafrost and Periglacial Press (Jhon Wiley & Sons): Hoboken, NJ, USA, 2005; Volume 16, pp. 209–216. [CrossRef]
19. Dorjgotov, D.; Orshih, N. (Eds.) Administration of Land Affairs, Geodesy and Cartography. In *Geographic Atlas of Mongolia*; Zurag Zuy Co. Ltd.: Ulaanbaatar, Mongolia, 2004; p. 61.
20. James, T.M. Temperature sensitivity and recruitment dynamics of Siberian larch (*Larix sibirica*) and Siberian spruce (*Picea obovate*) in northern Mongolia's boreal forest. *For. Ecol. Manag.* **2011**, *262*, 629–636. [CrossRef]
21. Kew Science: Plant of the World Online. Available online: https://powo.science.kew.org. (accessed on 27 August 2022).
22. Nandintsetseg, B.; Scott, J.; Goulden, C.E. Trends in extreme daily precipitation and temperature near Lake Hovsgol, Mongolia. *Int. J. Climatol.* **2007**, *347*, 341–347. [CrossRef]
23. Goulden, C.E.; Sitnikova, T.; Gelhaus, J.; Boldgiv, B. *The Geology, Biodiversity and Ecology of Lake Hovsgol (Mongolia)*; Backhuys Publishers Leiden, Backhuy Pub.: Liden, Netherlands, 2006; p. 525; ISBN 9057821621.
24. Krivonogov, S.K.; Sheinkman, V.S.; Mistruykov, A. Stages in the development of the Darhad dammed lake (Northern Mongolia) during the Late Pleistocene and Holocene. *Quat. Int.* **2005**, *136*, 83–94. [CrossRef]
25. Hayford, B.; Goulden, C.; Boldgiv, B. Spatial heterogeneity in macroinvertebrate density from Lake Hövsgöl, Mongolia. *J. Species Res.* **2013**, *2*, 159–166. [CrossRef]
26. Gillespie, A.R.; Burke, R.M.; Komatsu, G.; Bayasgalan, A. Late Pleistocene glaciers in Darhad Basin, northern Mongolia. *Quat. Res.* **2008**, *69*, 169–187. [CrossRef]

27. Brunello, A.J.; Molotov, V.C.; Dugherkhuu, B.; Goldman, C.; Khamaganova, E.; Strijhova, T.; Sigman, R. Lake Baikal: Lake Basin Management Initiative Experience and Lessons Learned Brief. In Proceedings of the Lake Basin Management Initiative Regional Workshop held at St. Michael's College in Vermont, USA, Colchester, VT, USA, 18–21 June 2003; p. 26.
28. Mongolian Meteorological Agency. *Murun Weather Station*; 2014.
29. Wikipedia. Available online: https://en.Wikipedia.org/wiki/Lake_Khövsgöl (accessed on 16 August 2022).
30. Sharkhuu, A.; Sharkhuu, N.; Etzelmüller, B.; Heggem, E.S.F.; Nelson, F.E.; Shiklomanov, N.I.; Goulden, C.E.; Brown, J. Permafrost monitoring in the Hovsgol mountain region, Mongolia. *J. Geophys. Res. Earth Surf.* **2007**, *112*, 1–11. [CrossRef]
31. Stefan, J. Über die Theorie der Eisbildung, insbesondere über die Eisbildung im Polarmeere. (The theory of ice formation, especially regarding ice formation in the Polar Sea). *Ann. Phys. Chem.* **1891**, *42*, 269–286. [CrossRef]
32. Smith, C.; Burn, C.; Tarnocai, C.; Sproule, B. Air and soil temperature relations along an ecological transect through the permafrost zones of northwestern Canada. In Proceedings of the Permafrost–7th International Conference, Yellowknife, Canada, 23–27 June 1998; Volume 55, pp. 1009–1015.
33. Woo, M.-k.; Arain, M.A.; Mollinga, M.; Yi, S. A two-directional freeze and thaw algorithm for hydrologic and land surface modelling. *Geophys. Res. Lett.* **2004**, *31*, L12501. [CrossRef]
34. Heggem, E.S.F.; Etzelmüller, B.; Anarmaa, S.; Sharkhuu, N.; Goulden, C.; Nandintsetseg, B. Spatial Distribution of Ground Surface Temperatures and Active Layer Depths in the Hovsgol Area, Northern Mongolia. *Permafr. Periglac. Process* **2006**, *17*, 357–369. [CrossRef]
35. Nelson, F.E.; Outcalt, S.I. A computational method for prediction and regionalization of permafrost. *Arct. Alp. Res.* **1987**, *19*, 279–288. [CrossRef]
36. National Astronomical Observatory. *Rika Nenpyo (Chronological Scientific Tables)*; Marizen Co. Ltd.: Tokyo, Japan, 2021; p. 1174; ISBN 978-4-621-30560-7.
37. Mackay, J.R. Active layer slope movement in a continuous permafrost environment, Garry Island, Northwest Territories, Canada. *Can. J. Earth Sci.* **1981**, *18*, 1666–1680. [CrossRef]
38. Mackay, J.R. Downward water movement into frozen ground, western arctic coast, Canada. *Can. J. Earth Sci.* **1983**, *20*, 120–134. [CrossRef]
39. Japan Society of Thermophysical Properties. *Thermophysical Properties Handbook*; Youkendo: Tokyo, Japan, 1990; p. 625.
40. Gula, J.; Peltier, W.R. Dynamical downscaling over the Great Lakes Basin of North America using the WRF regional climate model: The impact of the Great Lakes System on regional greenhouse warming. *J. Clim.* **2012**, *25*, 7723–7742. [CrossRef]
41. Notaro, M.; Holman, K.; Zarrin, A.; Fluck, E.; Vavrus, S.; Bennington, V. Influence of the Laurentian Great Lakes on regional climate. *J. Clim.* **2013**, *26*, 789–804. [CrossRef]
42. Bartunkova, K.; Sokol, Z.; Pop, L. Simulations of the influence of lake area on local temperature with the COSMO NWP model. *Atmos. Res.* **2014**, *147*, 51–67. [CrossRef]
43. Lang, J.; Ma, Y.; Li, Z.; Su, D. The impact of climate warming on lake surface heat exchange and ice phenology of different types of lakes on the Tibetan Plateau. *Water* **2021**, *13*, 634. [CrossRef]